

## PAPER DETAILS

TITLE: Estimation of the Daily Production Levels of a Run-of-River Hydropower Plant Using the Artificial Neural Network

AUTHORS: Hüseyin ALTINKAYA, Mustafa YILMAZ

PAGES: 62-72

ORIGINAL PDF URL: <https://dergipark.org.tr/tr/download/article-file/2848130>

# Estimation of the Daily Production Levels of a Run-of-River Hydropower Plant using the Artificial Neural Network

<sup>\*1</sup>Hüseyin ALTINKAYA, <sup>2</sup>Mustafa YILMAZ

<sup>1</sup>Department of Electrical and Electronics Engineering, Karabük University, Karabük, Türkiye, [haltinkaya@karabuk.edu.tr](mailto:haltinkaya@karabuk.edu.tr) 

<sup>1</sup>Department of Electrical Engineering, Faculty of Technology, Karabük University, Karabük, Türkiye, [mustafayilmaz@karabuk.edu.tr](mailto:mustafayilmaz@karabuk.edu.tr) 

## Abstract

Renewable energy sources, as well as the studies being conducted regarding these energy sources, are becoming increasingly important for our world. In this manuscript, the daily energy production level of a small (15 MW) run-of-river hydropower plant (RRHPP) was estimated using the artificial neural network (ANN) model. In this context, the model utilized both meteorological data and HPP-related data. The input parameters of the artificial neural network included the daily total precipitation, daily mean temperature, daily mean water vapour pressure, daily mean relative humidity, and the daily mean river water elevation at the hydropower plant, while the only output parameter consisted of the total daily energy production. For the ANN, data from the four years between 2017 and 2020 were used for training purposes, while data from the first eight months of 2021 were used for testing purposes. Ten different ANN networks were tested. A comparison of the ANN data with the real data indicated that the model provided satisfying results. The minimum error rate was 0.13%, the maximum error rate was 9.13%, and the mean error rate was 3.13%. Furthermore, six different algorithms were compared with each other. It was observed that the best results were obtained from the Levenberg-Marquardt algorithm. This study demonstrated that the ANN can estimate the daily energy production of a run-of-river HPP with high accuracy and that this model can potentially contribute to studies investigating the potential of renewable energies.

**Keywords:** Artificial Neural Network; Run-of-River Hydropower Plant; Renewable Energy

## 1. INTRODUCTION

In our ever-growing and developing world, the need for energy is constantly increasing. Nowadays, electricity inarguably represents the most commonly used and indispensable form of energy. Electric energy can be produced from fossil fuel sources such as coal, oil, and natural gas, and renewable energy sources such as water, wind, and solar energy. As fossil fuels are limited in supply (with most forms of fossil fuels expected to be depleted in less than 100 years) and contribute to environmental pollution, environment-friendly alternative energy sources are becoming increasingly important. In both Turkey and around the world, fossil fuels have a significant share in electricity production as compared to renewable energy sources. According to the report on the share of different energy sources in world electricity production in 2020, the share of hydroelectric power plants is 16% [1].

Renewable energy sources have a considerably smaller share in electricity production than fossil fuels. In Turkey, natural gas is the energy source with the largest share in electricity production, while hydropower-based sources rank second.

Turkey is a natural gas and oil importing country; this renders the effective use of hydro sources in Turkey even more important. Another noteworthy point is that as of the end of 2021, HPPs with dams have a 23.3% share in total installed power capacity. However, their share in total electricity production is only 12.3%. On the other hand, run-of-river HPPs have an 8.2% share in installed power capacity, and a 4.6% share in electricity production [2,3]. Based on these data, it is possible to see that most dam and run-of-river HPPs in Turkey are operating below capacity. The production capacity of HPPs is directly related to the quantity of water. Therefore, meteorological parameters, such as the amount of precipitation, needs to be taken into account. These parameters are even more important for run-of-river HPPs, which lack dams and use water directly.

An evaluation of the literature shows that studies regarding run-of-river HPPs and dam HPPs generally focus on topics such as production capacity of reservoir [4-6]; climate change potential effects on the run-of-river plant [7]; water flow management [8]; estimating the water collection capacity and the water elevation of dams [9,10]; determining the type of turbines most suitable for run-of-river plants

[11,12]; determining the optimal sizing of run-of-river plants; assessing the costs of small HPP projects [13-15]; management of the HPP [16-18]; and controlling HPPs with expert systems [19-22].

This study is genuine in terms of estimating the daily production amount of the RRHPP based on meteorological data. In the literature, we encountered a single study which modelled a dam HPP based on meteorological data [23]. However, no studies were encountered that estimated the production levels of run-of-river HPPs by using meteorological data.

In this respect, this manuscript intends to bring a new perspective to current studies conducted on run-of-river HPPs. The paper is organized as described below.

Chapter 1 provides an introduction to the research topic and the main objectives of the study. In chapter 2, the working principle of RRHPP is explained in detail. Section 3 presents technical data and information related exclusively to RRHPP. Chapter 4 offers a brief overview of artificial neural networks (ANN), which are used in the study to estimate the daily electricity generation level of RRHPP. In section 5, the methodology for using ANN to estimate daily electricity generation is explained in detail, and the results are presented and analyzed through tables and graphs. Finally, in chapter 6, the conclusion is presented along with suggestions for future studies.

## 2. WORKING PRINCIPLE OF THE RUN-OF-RIVER PLANTS

Both run-of-river and dam HPPs operate depending on some energy conversion stages. Firstly, the potential energy in water is converted into kinetic energy. Then, the obtained kinetic energy is converted into mechanical energy, and

eventually, the mechanical energy is converted into electrical energy.

The process of electrical energy production in most of the run-of-river plants is conducted as follows: firstly, water from the river is transferred to a waterway by the use of a weir or a regulator, and then, it is carried into the forebay through the waterway. Using the penstocks, stagnant water collected in the forebay is transferred to a turbine, thus, causing blades of the turbine to turn along with a generator rotor which is connected to the turbine with a shaft. Accordingly, the conversion of potential energy stored in the water into kinetic energy is carried out by the penstock; the conversion of kinetic energy into mechanical energy is carried out by the turbines; and the conversion of mechanical energy into electrical energy is carried out by the generator. After amplifying the electrical energy obtained by the generator using transformers, it is fed to power transmission lines. The working principle of run-of-river plants is illustrated in the diagram shown in Figure 1.

There are several equipment and intermediate stages used in the electricity production process in HPPs. Not going into details of electricity production process, we will be providing information about the alternators, turbines and power control systems considered to be one of the most important elements.

The kinetic energy of the water falling from a higher level to a lower level through the penstocks is captured by the turbines and their blades convert the obtained kinetic energy into mechanical energy. Based on flow rate as well as the pressure of the water which will rotate the turbine in a plant, the turbine type to be used is selected. The rotating part in all turbines is known to be rotor, whereas the non-moving part is known to be spiral casing. Currently, there are three turbine types being used: Kaplan, Francis, and Pelton turbines.

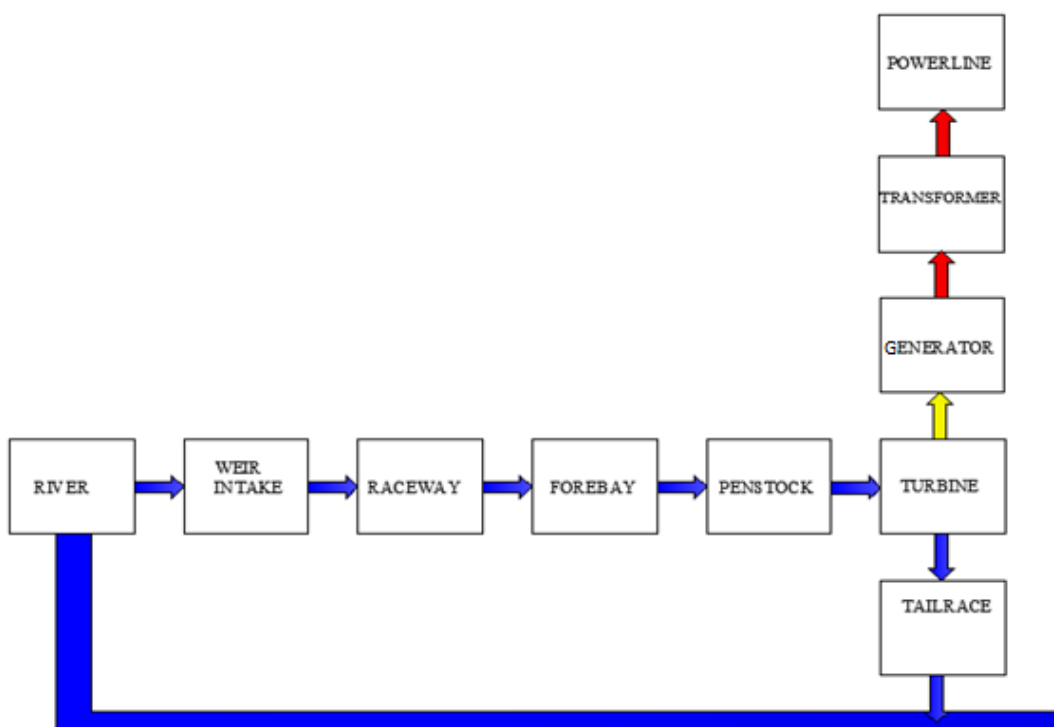


**Figure 1.** Energy production process in run-of-river plants.

According to the reference values, previously determined frequency and voltage values are continually adjusted and controlled. During the charging process of the generator, the turbine speed decreases. In order to bring the generator frequency and the turbine speed to the desired values, the water flow rate is increased by adjusting the valves and turbine wicket gates. Adjusting the valves and turbine wicket gates become necessary as the water flow rate is decreased in case of a decrease in generator charge. Nowadays, PID control systems are used to perform modern speed/rate controls. Such systems are being constantly monitored with the help of PLC-SCADA, and a database stores the relevant recorded data.

Depending on their power capacity, HPPs are classified as large capacity ( $> 50$  MW), small capacity (10-50 MW), mini capacity (0.1-10 MW), and micro capacity ( $< 0.1$  MW) HPPs.

The formulae for potential energy and kinetic energy are given as follows:

$$E_p = m \cdot g \cdot h \quad (1)$$

$$E_k = \frac{1}{2} \cdot m \cdot v^2 \quad (2)$$

where  $E_p$  represents potential energy (J);  $m$  represents the object's mass (kg);  $g$  represents the gravitational acceleration ( $9.81 \text{ m/s}^2$ );  $h$  represents height (m);  $E_k$  represents kinetic energy (J); and  $v$  represents speed (m/s). The electric power generated by HPPs is calculated using the formula below:

$$P = \rho \cdot g \cdot Q \cdot h \cdot \eta \quad (3)$$

where  $P$  represents electric power (W);  $\rho$  represents the specific density of water ( $1000 \text{ kg/m}^3$ );  $Q$  represents the flow rate of the water reaching the turbine ( $\text{m}^3/\text{s}$ );  $h$  represents the net falling height (elevation difference between the inlet and outlet, m); and  $\eta$  represents the system's efficiency (total efficiency comprising the

respective efficiencies of the penstock, turbine and generator, %). In case  $\rho$  is not used in the formula, the calculated power will be expressed in kW.

### 3. THE YALNIZCA RUN-OF-RIVER HYDROPOWER PLANT

Filyos Yalnizca Energy run-of-river HPP is situated in Karabük province located within Western Black Sea region of Turkey. The plant was inaugurated in September 2009 and has 15 MW installed power capacity consisting of three units with 5 MW power capacity each.

Yalnizca Hydropower Plant is situated on Filyos (Yenice) River and receives water from a 2 km waterway passing through a tunnel. The penstocks diameter of the plant is found to be 2.75 m, whereas the length is found to be 43 m. The water flow rate via the penstocks is observed to be  $25 \text{ m}^3$  per second. The water altitude of the forebay is 221.6 m, and the water altitude of tailwater channel is found to be 199.2 m. The falling height or the net head of the plant is observed to be 22 m, on average. The alternators or the generators have nominal power of 5100 kW. The voltage, nominal current, revolution speed and frequency are found to be 6.3 kV, 550 A, 333.3 rpm and 50 Hz, respectively. The afore-mentioned HPP uses Kaplan type horizontal-axis turbines. As seen in Figure 2, the fully automated plant is monitored and controlled with the SCADA system. Geographically, the HPP is located at 41.1633 parallel north and 32.5176 meridian east.

### 4. ARTIFICIAL NEURAL NETWORKS (ANN)

ANNs have been successfully used in learning, generalization, association, determining features classification and optimization. Using this technique, the information obtained from samples are recorded in the networks, and through the experiences, networks tend to give identical decisions in similar situations. Technically, the ANN, as its primary task, determines a set of outputs which meet input sets submitted to it [26].

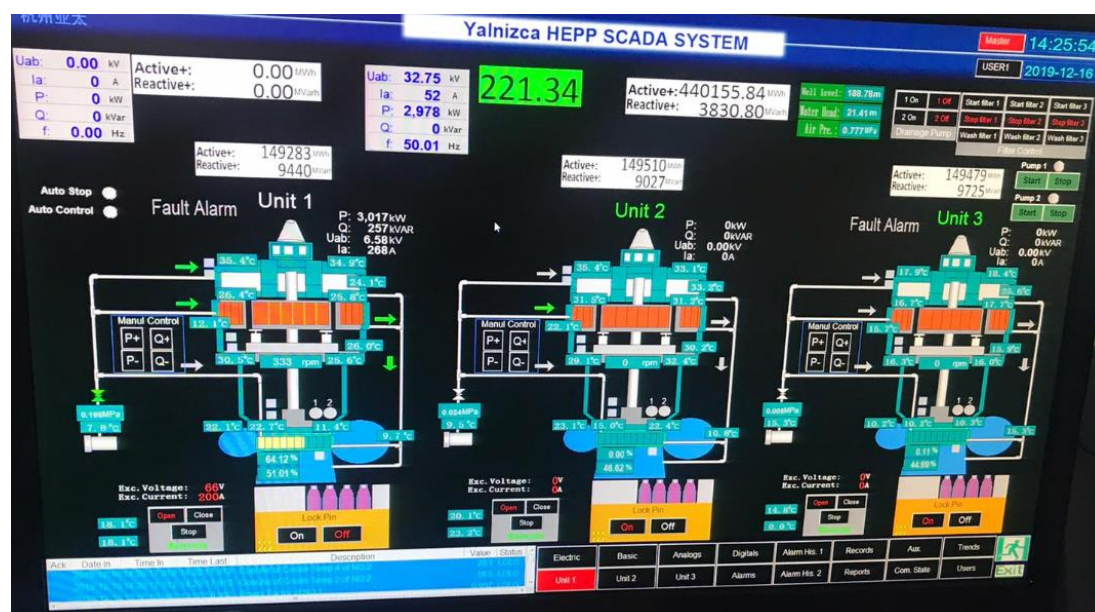
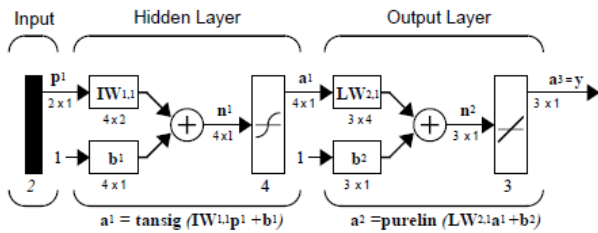


Figure 2. Yalnizca RRHPP SCADA main screen.

The ANN comprises artificial neural neurons. The neurons are assembled in three layers namely input, hidden and output layers as shown in Figure 3. Data obtained from the surrounding and fed into the input layer are transmitted to the hidden layer. Every process element in the layer consists of only one output, which is sent to each process elements present in the next layer. The information obtained from input layer is initially processed and then transferred to the next layer. In each layer, there might be more than one process and more than one hidden layer. The data received from hidden layers are processed in the output layer, and the generated outputs are sent to outside world by the network [24-26].



**Figure 3.** Architecture of feedforward network [27].

As our previous article [28] and the literature already provide a significant amount of information regarding the ANN, we will only provide the sigmoid function, RMSE,  $R^2$ , and MAPE equations in this context. Although there are several activation functions that can be considered, usually sigmoid function is used in the multilayer perceptron model. This function is expressed as follows [26].

$$f(x) = \frac{1}{1+e^{-x}} \quad (4)$$

The errors that occur during the training and test phases are referred to as root mean square errors (RMSE):

$$RMSE = \sqrt{\frac{\sum_{j=1}^n (t_j - o_j)^2}{n}} \quad (5)$$

Absolute fraction of variance ( $R^2$ ) and mean absolute percentage error (MAPE) are given as follows: [29-38]

$$R^2 = 1 - \left( \frac{\sum_{j=1}^n (t_j - o_j)^2}{\sum_{j=1}^n (t_j)^2} \right) \quad (6)$$

$$MAPE = \frac{1}{n} \sum_{j=1}^n \frac{|t_j - o_j|}{t_j} \times 100 \quad (7)$$

where,  $o$  is the output value,  $t$  is the target value and  $n$  is the pattern number.

The multilayer perceptron is part of the latent layered feed forward neural networks [39]. The performance of an ANN is significantly affected by the training algorithms, which optimize the biases and weights of the network based on the input-output pattern. Gradient methods and meta-heuristic methods are two commonly used types of training algorithms. Among the two, gradient methods are known to be effective, however, they have some drawbacks. One major disadvantage of gradient methods is that they can converge prematurely, and their performance depends

highly on the initial positions and parameters. Additionally, gradient methods can become trapped in local optima. Typically, gradient methods initiate the optimization process with a solution, thus guiding it to an optimum. Although the convergence is known to be fast, the solution's quality is greatly influenced by the initial solution. Mostly, the global optimum cannot be found using gradient method. Hence, meta-heuristic algorithms may be considered as alternative training algorithms. Different metaheuristic algorithms have been proposed by now. These algorithms can be listed as hybrid atom search optimization-simulated annealing (hASO-SA) [40], dragonfly [41], self-adaptive global best harmony search (SGHS) [42], cuckoo search algorithm [43], monarch butterfly optimization (IMBO) [44], particle swarm optimization and hybrid particle swarm optimization [45,46], grey wolf optimization [47, 48], dynamic group optimization [49], ant lion optimization [50], chimp optimization [51], grasshopper optimization [52], salp swarm [53], hybrid monarch butterfly and artificial bee colony optimization [54]. It is observed that the studies concentrate on the comparison of existing algorithms, improved algorithms or hybrid algorithms using various datasets.

## 5. ESTIMATION OF THE LEVEL OF ENERGY PRODUCTION WITH ANN

The Yalnızca run-of-river HPP is a plant located on the Yenice River, which is formed by the merging of the Araç and Soğanlı Streams. These two streams originate within the Kastamonu province, and then flow through the Karabük province. The Araç and Soğanlı Streams cover a distance of approximately 90 km before reaching the power plant. The watershed areas of the Araç and Soğanlı Streams are 2843 km<sup>2</sup> and 5102 km<sup>2</sup>, respectively. The amount of water reaching the plant is directly associated with the water flow of these two streams, which, in turn, are closely related to the meteorological parameters in the provinces of Karabük and Kastamonu.

For this reason, while developing the ANN architecture, the input parameters of the model included daily total precipitation, daily mean temperature, daily mean water vapour pressure and daily mean relative humidity for both provinces, as well as daily mean river water elevation at the hydropower plant. On the other hand, the only output parameter of the model consisted of the total daily energy production. Meteorological data were obtained from the Provincial Meteorology Directorates of Karabük and Kastamonu, which are branches of the General Directorate of Meteorology, while data regarding river water elevation and energy production levels of the power plant were obtained from the Yalnızca power plant. Water elevation data was transferred to the power plant by a GPRS system located 5 km upstream on the river. Data obtained during the period between 2017 and 2020 were used as training data for the ANN, while data from the first eight months of 2021 were used for testing purposes. Days during which technical issues at the power plant and/or meteorology centers caused data loss were not taken into consideration. Such days with data loss represented less than 3% of the total number of days.



The obtained data were normalized in such a way to have values ranging from 0.1 and 0.9. The formula used for normalization is given as follows:

$$V_N = 0.8 \times \left( \frac{V - V_{min}}{V_{max} - V_{min}} \right) + 0.1 \quad (8)$$

Where;  $V_N$  is the normalized value,  $V_{min}$  is the minimum value,  $V$  is the original value, and  $V_{max}$  is the maximum value. To determine the original value obtained from the normalized value, the formula used is given as follows:

$$V = \frac{V_N(V_{max} - V_{min}) - 0.1V_{max} + 0.9V_{min}}{0.8} \quad (9)$$

Tables 1 and 2 provide examples of non-normalized and normalized data sets.

**Table 1.** A sample of non-normalized dataset in Jan 2020.

Date	Krb DTP (mm)	Krb DMT (°C)	Krb DMWVP (hpa)	Krb DMRH (%)	Kst DTP (mm)	Kst DMT (°C)	Kst DMWVP (hpa)	Kst DMRH (%)	DMRWE (cm)	Prod (MWh)
1	0.2	4.2	7.5	92	0	3.4	7.4	97.6	57.46	33.25
2	0.8	2.6	6.3	88.6	0.4	1	5.7	88	64.29	25.53
3	0	1.2	5.6	86	0	0.3	5.5	89.5	65.46	36.50
4	0	1.3	5.8	89.3	0	0	5.7	93.6	67.71	41.58
5	1.4	2.3	6.5	93.9	0.3	2.1	5.8	85.9	64.5	38.17
6	0	0.8	6	96.5	0	-0.6	5.6	95.5	69.54	42.15
7	5.7	2.5	7	98.5	0.1	2.1	6.8	98.4	69.12	42.38
8	3.8	4.1	7.9	96.5	3.3	2.9	7.2	99	65.83	36.36
9	1.8	1.3	5.7	86.5	2	0.7	5.7	90	68.29	40.46
10	0	1.4	5.4	81.8	0	-1.1	5.1	90.5	69.12	41.14

**Table 2.** A sample of normalized dataset in May 2020

Date	Krb DTP (mm)	Krb DMT (°C)	Krb DMWVP (hpa)	Krb DMRH (%)	Kst DTP (mm)	Kst DMT (°C)	Kst DMWVP (hpa)	Kst DMRH (%)	DMRWE (cm)	Prod (MWh)
1	0.1049	0.1000	0.2810	0.1000	0.1196	0.1024	0.1147	0.1000	0.1073	0.1881
2	0.7232	0.6370	0.5994	0.6083	0.6370	0.6326	0.6238	0.6348	0.6083	0.6525
3	0.4629	0.6155	0.5041	0.4835	0.5536	0.5330	0.5206	0.5619	0.5948	0.5660
4	0.2695	0.5496	0.5735	0.4316	0.5283	0.5207	0.4805	0.5396	0.6388	0.4680
5	0.1000	0.3433	0.4023	0.1000	0.1737	0.1000	0.1479	0.1000	0.1000	0.1000
6	0.6811	0.6347	0.5800	0.6368	0.6305	0.6095	0.6179	0.6326	0.6474	0.6811
7	0.5889	0.7123	0.5444	0.5296	0.5938	0.5938	0.5790	0.5938	0.6037	0.6086
8	0.4938	0.7523	0.6538	0.5185	0.6169	0.6662	0.6169	0.6046	0.5677	0.5062
9	0.2059	0.2039	0.2137	0.2196	0.2118	0.2098	0.2176	0.2176	0.2216	0.2294
10	0.2466	0.2279	0.2567	0.2735	0.2546	0.2642	0.2651	0.2638	0.2725	0.2914

**Table 3.** The number of hidden layer(s) and neurons of the networks

Networks	Hidden Layer(s) Number	Neurons Number in the First Hidden Layer	Neurons Number in the Second Hidden Layer
Network 1	1	10	-
Network 2	1	15	-
Network 3	1	20	-
Network 4	1	25	-
Network 5	1	30	-
Network 6	2	13	5
Network 7	2	21	3
Network 8	2	15	4
Network 9	2	16	2
Network 10	2	30	3

In the study, the daily total precipitation was coded as DTP, the daily mean temperature as DMT, the daily mean water vapour pressure as DMWVP, the daily mean relative humidity as DMRH, and the daily mean river water elevation as DMRWE. Krb was used as the abbreviation for Karabük, and Kst was used as the abbreviation for Kastamonu.

The network type was chosen as feed-forward backpropagation. Among different algorithms as well as intermediate layers, the best results were observed to be obtained from the algorithm known as Levenberg-Marquardt (LM) having two hidden layers. The transfer functions selected were Tansig (Tan-sigmoid transfer function), Purelin (linear transfer function) and Logsig (Log-sigmoid transfer function), and using these three transfer functions, similar results were obtained. The ANN was trained using MATLAB software.

There is no agreed rule in literature for determining the hidden layer and neuron numbers in these layers. However, researchers have proposed some approaches regarding the determination of these afore-mentioned numbers of hidden layers and neurons [55-59].

The ten networks which have different hidden layers and/or neurons were tested. First network had one hidden layer with 10 neurons; the second had one hidden layer with 15 neurons; the third had one hidden layer with 20 neurons; the fourth had one hidden layer with 25 neurons; the fifth had one hidden layer with 30 neurons; the sixth network comprised two hidden layers having 13 neurons and 5 neurons in the first and in the second layer, respectively; the seventh network comprised two hidden layers having 21 neurons and 3 neurons in the first and in the second layer, respectively; the eighth network comprised two hidden layers having 15 neurons and 4 neurons in the first and in the second layer, respectively; the ninth network comprised two hidden layers having 16 neurons and 2 neurons in the first and in the second layer, respectively; the tenth network comprised two hidden layers having 30 neurons and 3 neurons in the first and in the second layer, respectively. The number of hidden layers and neurons of the networks are shown in Table 3.

Results obtained from the networks with one hidden layer were close to each other, while results from the networks with two hidden layers were quite different from each other. Statistical values of the ten networks are presented in Table 5.

Among the artificial neural networks trained using varying architectures, the ANN architectures which provided the best, the second-best and the worst results and consisted of two hidden layers having 16 and 2 neurons in the first and in the second layer (the ninth network), respectively; two hidden layers with 13 neurons in the first layer and 5 neurons in the second layer (the sixth network); two hidden layers with 30 neurons in the first layer and 3 neurons in the second layer (the tenth network) were used, respectively. Architecture of the second-best and the best networks are illustrated in Figures 4 and 5.

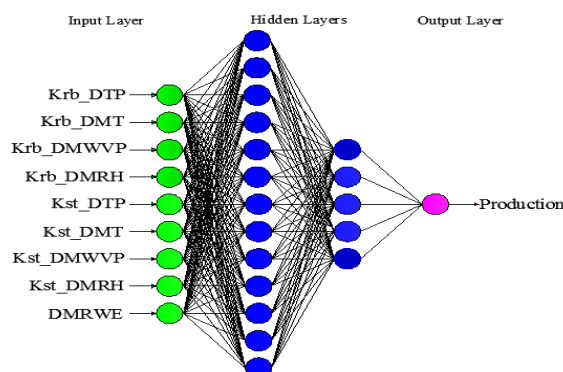


**Figure 4.** Architecture of the second-best ANN.

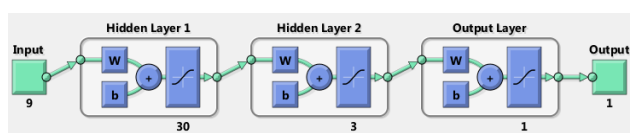


**Figure 5.** View of the best ANN in Matlab.

The common practice while training multi-layer networks using MATLAB environment is to initially split the data into three subsets as follows. The first subset used in order to compute the gradient as well as to update the network biases and weights, is the training set. The second subset is known to be the validation set. During the training process, the validation set error, which normally decreases in the initial phase of the training, is monitored. However, the validation set error starts increasing when the data are overfitted by the network. The network biases and weights are recorded at the minimum value of validation set error. While training the networks, test set error is not used. The test set error is used merely to compare different models [24]. Figure 6 shows the best (tenth) neural network regression results. These regression results represent the best results from 30 different trials using different random initial weights in each trial.

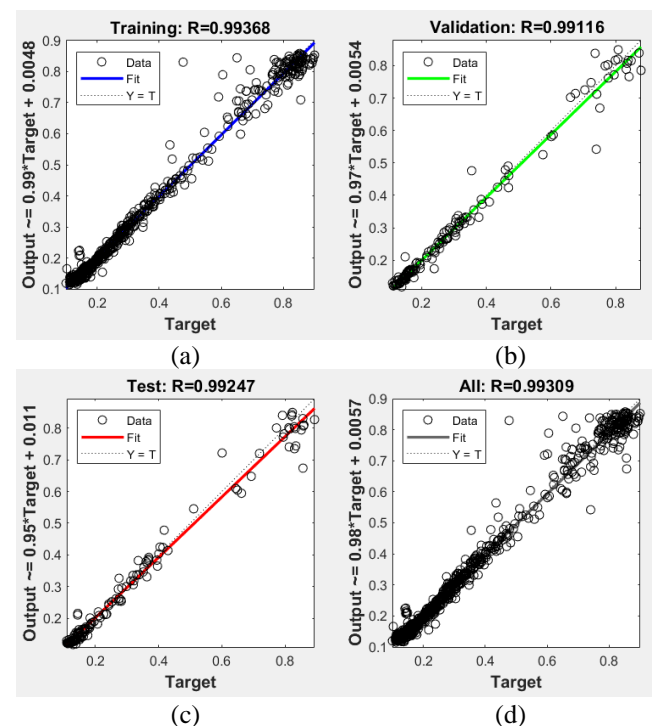


**Figure 6.** The tenth neural network regression results: (a) Training, (b) Validation, (c) Test, (d) All

For instance, Figures 7-9 are the graphical representations of the daily production levels in Jan, Apr and Aug 2021 respectively.

When actual values and ANN-derived values are compared, the min, max and mean error rates for daily production levels in January are found to be 0.41% (on Jan 4), 7.25% (on Jun 29), and 3.41%, respectively; for daily production levels in February, the min, max and mean error rates are 0.65% (on Feb 11), 5.41% (on Feb 20), and 3.25%, respectively; for daily production levels in March, the min, max and mean error rates are 0.61% (on Mar 13), 6.44% (on Mar 5), and 3.28%, respectively; for daily production levels in April, the min, max and mean error rates are 0.13% (on Apr 21), 5.12% (on Apr 28), and 3.48%, respectively; for daily production levels in May, the min, max and mean error rates are 1.03% (on May 7), 4.73% (on May 21), and 2.48%, respectively; for daily production levels in June, the min,

max and mean error rates are 1.22% (on Jun 3), 5.64% (on Jun 23), and 2.91%, respectively; for daily production levels in July, the min, max and mean error rates are 0.58% (on Jul 6), 9.13% (on Jul 20), and 4.90%, respectively; and for daily production levels in August, the min, max and mean error rates are determined as 0.18% (on Aug 7), 3.16% (on Aug 16), and 1.36%, respectively. The error rates of daily production levels for first eight months of 2021 are given in Table 4.

**Table 4.** Error rates by months

Months	Min (%)	Max (%)	Mean (%)
Jan	0.41	7.25	3.41
Feb	0.65	5.41	3.25
Mar	0.61	6.44	3.28
Apr	0.13	5.12	3.48
May	1.03	4.73	2.48
Jun	1.22	5.64	2.91
Jul	0.58	9.13	4.90
Aug	0.18	3.16	1.36

The statistical values for ANN output of each network for training and test data are shown in Table 5. When MAPE values are considered, the ninth network has the highest

MAPE values, while the tenth network has the lowest MAPE values. On the other hand, MAPE values of the networks with one hidden layer are usually close to each other and are observed to be in 5-6 range. When RMS,  $R^2$  and MAPE values are observed in Table 5, the tenth network is found to be the best network. It is clearly indicated in Table 5 that the accurate statistical values of the process represent the tenth ANN model, and these values may predict daily production levels of ANN.

In addition, five different algorithms apart from the LM algorithm are selected in the Matlab environment, and the training and test results were compared with the same data set. These algorithms are BFG (BFGS Quasi-Newton), RP (Resilient Backpropagation), SCG (Scaled Conjugate Gradient), CGB (Conjugate Gradient with Powell/Beale Restarts), GDX (Variable Learning Rate Backpropagation). The results obtained are given in Table 6. It is clearly seen that the best results among these algorithms are obtained from the LM algorithm. The results in the table show the best results from 30 different trials using different random initial weights in each trial. The statistical values for ANN output of each algorithm for training and test data are shown in Table 7.

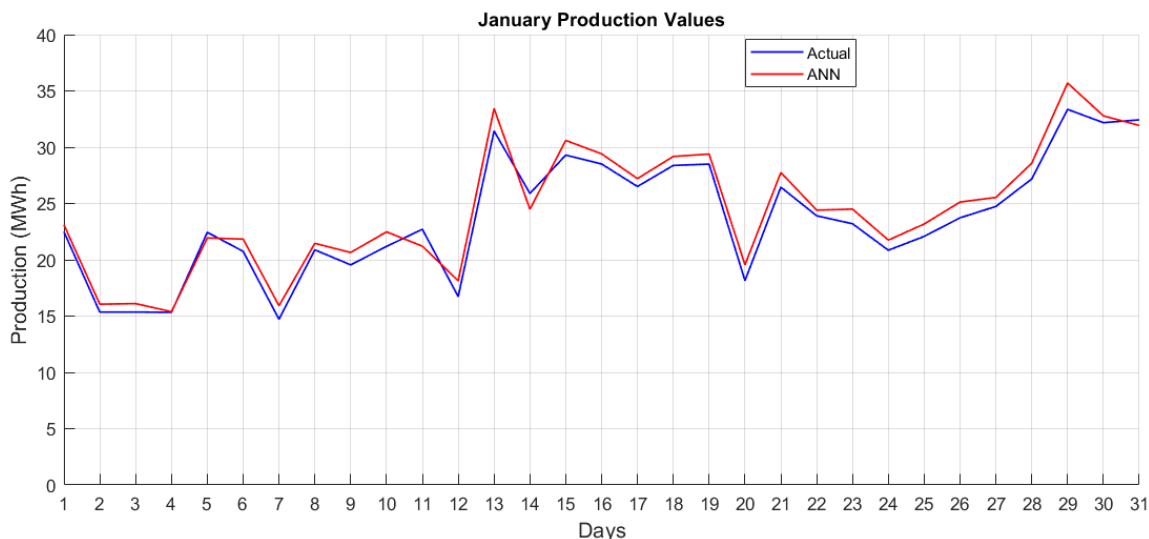


**Figure 7.** Daily production levels of Jan 2021.

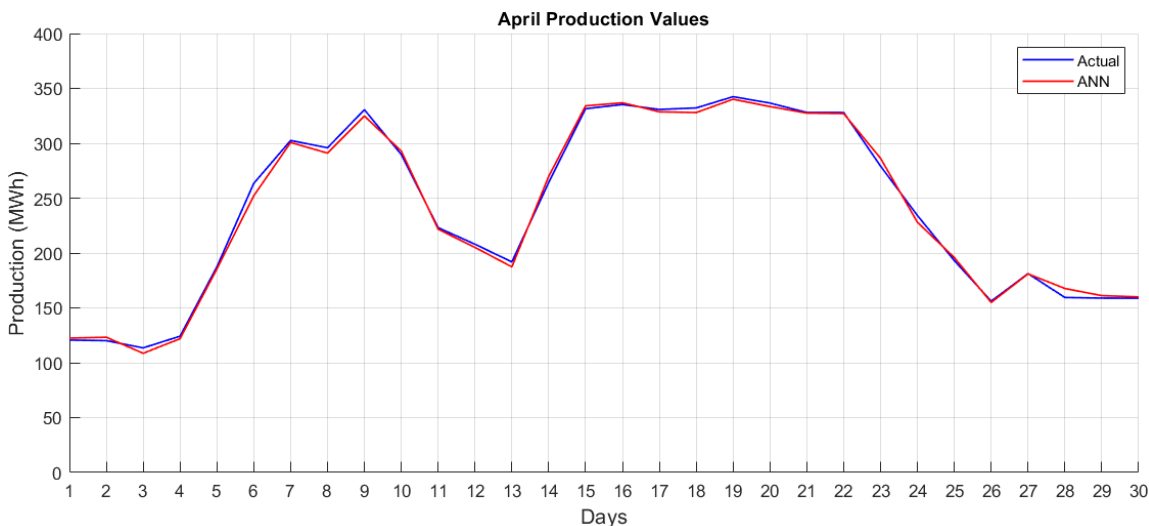


**Figure 8.** Daily production levels of Apr 2021.



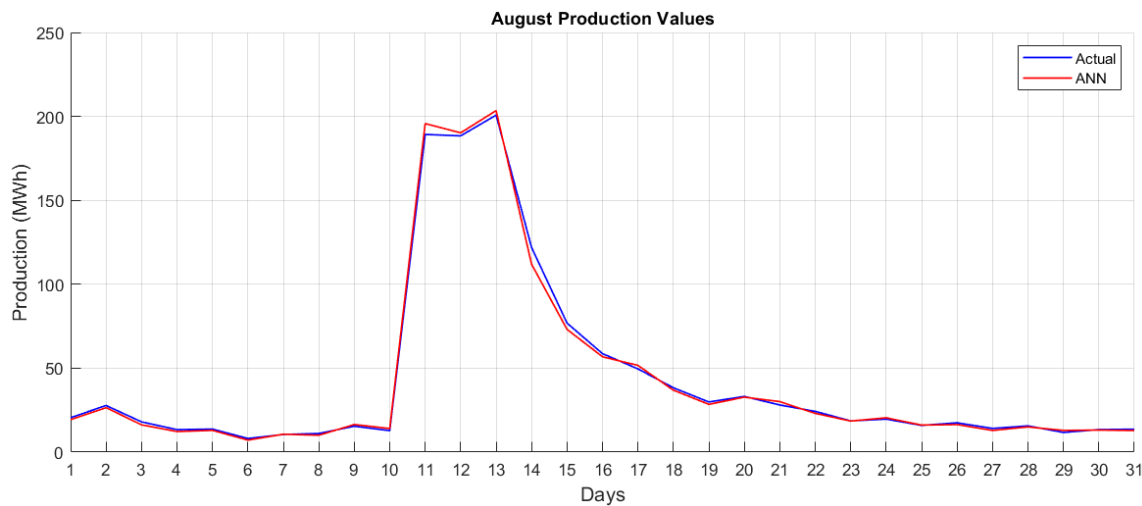


**Figure 9.** Daily production levels of Aug 2021.

**Table 5.** Statistical values of the networks

Networks	RMS training	R <sup>2</sup> training	MAPE training (%)	RMS test	R <sup>2</sup> test	MAPE test (%)
Network 1	0.030271	0.994243	5.781309	0.066026	0.987400	9.095667
Network 2	0.033671	0.992582	5.811954	0.049437	0.992936	5.891360
Network 3	0.036420	0.991917	6.659378	0.046493	0.993752	6.165773
Network 4	0.025555	0.995609	5.886150	0.053759	0.991647	6.117854
Network 5	0.032906	0.993328	5.644807	0.055559	0.991078	6.733954
Network 6	0.024699	0.996333	5.538720	0.050675	0.992578	6.432624
Network 7	0.035923	0.992301	6.317151	0.052849	0.991928	5.794437
Network 8	0.081876	0.960463	10.387326	0.070208	0.985754	6.404879
Network 9	0.137353	0.931282	20.617585	0.162874	0.915841	23.893251
Network 10	0.009243	0.999946	2.873423	0.011517	0.999546	3.217632

**Table 6.** The algorithms regression results

Algorithm	Training	Validation	Test	All
LM (Levenberg-Marquardt)	R=0.99368	R=0.99116	R=0.99247	R=0.99309
BFG (BFGS Quasi-Newton)	R=0.98662	R=0.95406	R=0.98945	R=0.98153
RP (Resilient Backpropagation)	R=0.98071	R=0.98521	R=0.98393	R=0.98211
SCG (Scaled Conjugate Gradient)	R=0.98154	R=0.99055	R=0.98066	R=0.98264
CGB (Conjugate Gradient with Powell/Beale Restarts)	R=0.98295	R=0.98473	R=0.9792	R=0.98258
GDX (Variable Learning Rate Backpropagation)	R=0.97293	R=0.98045	R=0.98026	R=0.97539

**Table 7.** Statistical values of the algorithms

Algorithm	RMS training	R <sup>2</sup> training	MAPE training (%)	RMS test	R <sup>2</sup> test	MAPE test (%)
LM	0.009243	0.999946	2.873423	0.011517	0.999546	3.217632
BFG	0.008271	0.999453	3.689555	0.037236	0.992544	3.811289
RP	0.008036	0.999168	3.745125	0.037384	0.992436	3.853741
SCG	0.008145	0.999237	3.692573	0.038136	0.992158	3.872589
CGB	0.008243	0.999316	3.686782	0.038265	0.991768	3.886723
GDX	0.007736	0.998785	4.875891	0.038244	0.991835	3.885692

## 6. CONCLUSION

This study employed Artificial Neural Network (ANN) to estimate the daily production level of a run-of-river HPP based on meteorological data. A comparison of the ANN and the real data indicated that the model provides fairly satisfying results. The minimum error rate was 0.24%, the

maximum error rate was 14.83%, and the mean error rate was 4.15%. The days with the highest error rates were observed for several days after very high daily total precipitation values occurred in Karabük and/or Kastamonu. We believe that these high precipitation days in these provinces were associated with highly variable quantities of water (and water flow), which in turn led to

significant variability in the production levels of power plant.

We hope that the estimation of the daily energy production of a run-of-river hydropower plant based on meteorological data will bring a new approach and perspective. It was observed that ANNs can be successfully implemented in the modelling of complex and non-linear systems. Most hydropower plants are facilities with considerably high initial setup costs. Thus, in countries such as Turkey that make significant investments in run-of-river hydropower plants, the ANN approach could contribute to the conduct of the effective feasibility studies before investment decisions, and also to correct decision-making processes that minimize the loss of time and funds.

In future studies, meta-heuristic algorithms will be used in the training of artificial neural networks. The data will be analyzed with different techniques. Also, we plan to develop a new ANN model that will allow for the estimation of a power plant's efficiency and increase the efficiency of turbines. In this context, we are also planning to develop an on-line hybrid system that will operate in integration with the PID control system. In addition, we will consider performing similar modelling activities with the ANN for run-of-river hydropower plants in other regions, so that we may compare data for different plants, and further test the reliability of the model.

#### ACKNOWLEDGMENT

We, as authors, would like to express our sincere gratitude to the Filyos Energy Yalnızca Power Plant, the General Directorate of Meteorology, the Provincial Meteorology Directorates of Karabük and Kastamonu, and the Karabük State Water Work (DSİ) for providing us with the necessary data and for their invaluable contributions and assistance.

**Author contributions:** Hüseyin Altinkaya: Concept, Literature review, Data collection, Software, Writing-Review & Editing, Analysis of results, Mustafa Yılmaz: Software, Writing-Review & Editing, Analysis of results, Investigation.

**Conflict of Interest:** No conflict of interest was declared by the authors.

**Financial Disclosure:** The authors declared that this study has received no financial support.

#### REFERENCES

- [1] WED, World Energy Data, <https://www.worldenergydata.org/world-electricity-generation/>
- [2] TEİAŞ, Turkish Electricity Transmission Corporation, <https://www.teias.gov.tr/tr-TR/aylik-elektrik-uretim-tuketim-raporlari>
- [3] TEİAŞ, Turkish Electricity Transmission Corporation, <https://www.teias.gov.tr/tr-TR/kurulu-guc-raporlari>
- [4] Fereidoon M., Najimi M., Khorasani, G., Simulation of hydropower systems operation using artificial neural network, *International Journal of Emerging Science and Engineering*, Volume-1, Issue-12, (2013) 86-89.
- [5] Yadav D., Sharma V., Artificial neural network based hydroelectric generation modelling. *International Journal of Applied Engineering Research*, Volume-1, No-3, (2010) 343-359.
- [6] Kuriqi A., Antonio NP., Ward AS., Garrote L., Flow regime aspects in determining environmental flows and maximising energy production at run-of-river hydropower plants, *Applied Energy*, 256 (2019) 113980.
- [7] Brito MA., Rodriguez DA., Junior VLC., Vianna JNS., The climate change potential effects on the run-of-river plant and the environmental and economic dimensions of sustainability, *Renewable and Sustainable Energy Reviews*, 147 (2021) 111238 1-21.
- [8] Gerini F., Vagnoni E., Cherkaoui R., Paolone M., Improving frequency containment reserve provision in run-of-river hydropower plants, *Sustainable Energy, Grids and Networks*, 28 (2021) 100538 1-12.
- [9] Csiki, S.J.C., & Rhoads B.L., Influence of four run-of-river dams on channel morphology sediment characteristics in Illinois, USA. *Geomorphology*, 206, (2014) 215–229.
- [10] Nwobi-Okoyea, C.C., & Igboanugob, A.C., (2013). Predicting water levels at Kainji dam using artificial neural network. *Nigerian Journal of Technology*, 32, 129-136.
- [11] Sharma, H., Singh, J., Run off river plant: Status and prospects, *International Journal of Innovative Technology and Exploring Engineering*, Volume-3, Issue-2, (2013) 210-213.
- [12] Özdemir MS., Dalcı A., Ocak C., Run of river Hydroelectric Power Plants and Turbine-Generators Used in These Power Plants, *Müh. Bil. Ve Araş. Dergisi* 2(2) (2020) 69-75.
- [13] Anagnostopoulos, J.S., Papantonis D.E., Optimal sizing of a run-of-river small hydropower plant, *Energy Conversion and Management*, 48, (2007) 2663–2670.
- [14] Mishra, S., Singal, S.K. & Khatod D.K., Optimal installation of small hydropower plant—A review, *Renewable and Sustainable Energy Reviews*, 15, (2011) 3862-3869.
- [15] Singal, S.K., Saini, R.P., Raghuvanshi C.S., Analysis for cost estimation of low head run-of-river small hydropower schemes, *Energy for Sustainable Development*, 14, (2010) 117-126.
- [16] Ardizzon, G., Cavazzini, G. & Pavesi, G., A new generation of small hydro and pumped-hydro power plants: Advances and future challenges, *Renewable and Sustainable Energy Reviews*, 31, (2014) 746-761.

- [17] Kumar, D. & Katoch, S.S., Sustainability indicators for run of the river (RoR) hydropower projects in hydro rich regions of India, *Renewable and Sustainable Energy Reviews*, 35, (2014) 101-108.
- [18] Molina J.M., Isasi, P., Berlanga, A. & Sanchis A., Hydroelectric power plant management relying on neural networks and expert system integration, *Engineering Applications of Artificial Intelligence*, 13, (2000) 357-369.
- [19] Dumur, D., Libaux A. & Boucher, P., Robust control for a Basse-Isere run-of-river cascaded hydro-electric plants. *Proceedings of the 2001 IEEE International Conference on Control Applications* September 5-7, Mexico City, Mexico, (2001). 1083-1088.
- [20] Kishor, N., Nonlinear predictive control to track deviated power of an identified NNARX model of a hydro plant, *Expert Systems with Applications*, 35 (2008)1741–1751.
- [21] Pérez-Díaz, J.I., Fraile-Ardanuy J., Neural networks for optimal operation of a run-of-river adjustable speed hydro power plant with axial-flow propeller turbine, *16th Mediterranean Conference on Control and Automation* Congress Centre, Ajaccio, France, 25-27 June, (2008) 309-314
- [22] Salhi, I., Doubabi, S., Essounbouli, N. & Hamzaoui, A., Frequency regulation for large load variations on micro-hydro power plants with real-time implementation. *International Journal of Electrical Power & Energy Systems*, 60 (2014) 6-13.
- [23] İnallı, K., Işık, E., Dağtekin, İ., The prediction of efficiency and production parameters in Karakaya hpp using the artificial network. *Dicle University Engineering Faculty Journal*, 5 (2014) 59-68.
- [24] Beale, M. H., Hagan, M. T., & Demuth, H. B. (2013). *Neural network toolbox user's guide*. MathWorks, Technical Support.
- [25] Nabiye V.V. (2005). *Artificial Intelligence*. Seckin publishing.
- [26] Öztemel E. (2003). *Artificial Neural Networks*. Seckin publishing.
- [27] <https://www.mathworks.com/help/deeplearning/ug/multilayer-neural-network-architecture.html>
- [28] Altinkaya, H., Orak İ.M. & Esen İ., Artificial neural network application for modeling the rail rolling process, *Expert Systems with Applications*, 41 (2014) 7135–7146.
- [29] Canakci, M., Ozsezen, A.N., Arcaklioglu, E., & Erdil, A. Prediction of performance and exhaust emissions of a diesel engine fuelled with biodiesel produced from waste frying palm oil, *Expert Systems with Applications*, 36 (2009) 9268-9280.
- [30] Koca, A., Oztop, H.F., Varol, Y., & Koca, G.O., Estimation of solar radiation using artificial neural networks with different input parameters for Mediterranean region of Anatolia in Turkey, *Expert Systems with Applications*, 38 (2011) 8756-8762.
- [31] Ozgoren, M., Bilgili, M., & Sahin, B., Estimation of global solar radiation using ANN over Turkey. *Expert Systems with Applications*, 39 (2012) 5043-5051.
- [32] Ekinci F., YSA ve ANFIS Tekniklerine Dayalı Enerji Tüketim Tahmin Yöntemlerinin Karşılaştırılması, *Düzce Üniversitesi Bilim ve Teknoloji Dergisi*, 7 (2019) 1029-1044.
- [33] Gündoğdu A., Çelikel R., ANN-Based MPPT Algorithm for Photovoltaic Systems, *Turkish Journal of Science & Technology* 15(2), (2020)101-110.
- [34] Kocaarslan İ., Akcay MT., Akgündoğdu A., Tiryaki H., Comparison of ANN and ANFIS Methods for the Voltage-Drop Prediction on an Electric Railway Line, *Electrica* (2018); 18(1): 26-35.
- [35] Işık H., Şeker M., Yapay Sinir Ağı (YSA) Kullanarak Farklı Kaynaklardan Türkiye’de Elektrik Enerjisi Üretim Potansiyelinin Tahmini, *Journal of Computer Science*. (2021) pp. 304-311, <http://doi.org/10.53070/bbd.991039>
- [36] Uzlu E., Estimates of hydroelectric energy generation in Turkey with Jaya algorithm-optimized artificial neural networks, *GU J Sci, Part C*, 9(3): 446-462 (2021).
- [37] Mustafa Şeker. Yapay Sinir Ağı (YSA) Kullanılarak Meteorolojik Verilere Dayalı Solar Radyasyon Tahmini, *DEÜ FMD* 23(69), 923-935, (2021).
- [38] Ilaboya, I.R and Igbinedion O. E. Performance of Multiple Linear Regression (MLR) and Artificial Neural Network (ANN) for the Prediction of Monthly Maximum Rainfall in Benin City, Nigeria, *International Journal of Engineering Science and Application*, Vol. 3, No. 1, (2019).
- [39] Haykin, S.: *Neural Networks: A Comprehensive Foundation*. Prentice Hall PTR, Upper Saddle River (1999).
- [40] Eker, E., Kayri, M., Ekinci, S., İzci, D., A New Fusion of ASO with SA Algorithm and Its Applications to MLP Training and DC Motor Speed Control, *Arabian Journal for Science and Engineering*, 46, (2021) 3889–3911.
- [41] Gülcü, Ş., Training of the feed forward artificial neural networks using dragonfly algorithm, *Applied Soft Computing*, 124, (2022) 109023.
- [42] Kulluk, S., Ozbakir, L., Baykasoglu, A., Training neural networks with harmony search algorithms for classification problems, *Eng. Appl. Artif. Intell.* 25 (2012) 11–19.
- [43] Valian, E., Mohanna, S., Tavakoli, S., Improved cuckoo search algorithm for feedforward neural network training, *Int. J. Artif. Intell. Appl.* 2 (2011) 36–43.
- [44] Faris, H., Aljarah, I., Mirjalili, S., Improved monarch butterfly optimization for unconstrained global search and neural network training, *Appl. Intell.* 48 (2018) 445–464.

- [45] Erdoğan, F., Gülcü, S., Training of artificial neural networks using meta heuristic algorithms, in: The International Aluminium-Themed Engineering and Natural Sciences Conference (IATENS19), Konya, Turkey, (2019), 124–128.
- [46] Xu, J., Yan, F., Hybrid Nelder–Mead algorithm and dragonfly algorithm for function optimization and the training of a multilayer perceptron. *Arab. J. Sci. Eng.* 44, (2019) 3473–3487.
- [47] Mirjalili, S., How effective is the grey wolf optimizer in training multi-layer perceptrons, *Appl. Intell.* 43 (2015) 150–161.
- [48] Zhang, X., Wang, X., Chen, H., Wang, D., Fu, Z., Improved GWO for large-scale function optimization and MLP optimization in cancer identification. *Neural Comput. Appl.* 32, (2020) 1305–1325.
- [49] Tang, R., Fong, S., Deb, S., Vasilakos, A.V., Millham, R.C., Dynamic group optimisation algorithm for training feed-forward neural networks, *Neurocomputing* 314 (2018) 1–19.
- [50] Heidari, A.A.; Faris, H.; Mirjalili, S.; Aljarah, I.; Mafarja, M.: Ant lion optimizer: theory, literature review, and application in multi-layer perceptron neural networks. In: Mirjalili, S., Song Dong, J., Lewis, A. (eds.) *Studies in computational intelligence*, pp. 23–46. Springer International Publishing, Cham (2020).
- [51] Khishe, M.; Mosavi, M.R., Classification of underwater acoustical dataset using neural network trained by Chimp Optimization Algorithm. *Appl. Acoust.* 157, (2020) 107005.
- [52] Heidari, A.A., Faris, H., Aljarah, I., Mirjalili, S., An efficient hybrid multilayer perceptron neural network with grasshopper optimization. *Soft. Comput.* 23, (2019) 7941–7958.
- [53] Khishe, M., Mohammadi, H., Passive sonar target classification using multi-layer perceptron trained by salp swarm algorithm. *Ocean Eng.* 181, (2019) 98–108.
- [54] Ghanem, W.A.H.M., Jantan, A., Training a neural network for cyberattack classification applications using hybridization of an artificial bee colony and monarch butterfly optimization. *Neural Process. Lett.* 51, (2020) 905–946.
- [55] Huang, G. B., Babri, H. A., Upper bounds on the number of hidden neurons in feed forward networks with arbitrary bounded nonlinear activation functions. *IEEE Transactions on Neural Networks*, 9(1) (1998).
- [56] Huang, S. C., Huang, Y. F. Bounds on the number of hidden neurons in multilayer perceptrons, *IEEE Transactions on Neural Networks*, 2(1), (1991) 47–55.
- [57] Karsoliya, S., Approximating number of hidden layer neurons in multiple hidden layer BPNN architecture. *International Journal of Engineering Trends and Technology*, 3(6), 714–717. ISSN: 2231-5381 (2012).
- [58] Khaw, J. F. C., Lim, B. S., & Lim, L. E. N., Optimal design of neural networks using the Taguchi method. *Neurocomputing*, 7 (1994) 225–245.
- [59] Panchal, G., Ganatra, A., Kosta, Y. P., & Panchal, D., Behaviour Analysis of Multilayer Perceptrons with Multiple Hidden Neurons and Hidden Layers, *International Journal of Computer Theory and Engineering* 3(2). ISSN: 1793-8201 (2011).